Short- and Medium-Wave Infrared Drying of Cantaloupe (*Cucumis melon* L.) Slices: Drying Kinetics and Process Parameter Optimization

Antai Chang [1,2], Xia Zheng [1,2,*], Hongwei Xiao [3], Xuedong Yao [1,2], Decheng Liu [1,2], Xiangyu Li [1,2] and Yican Li [1,2]

1 College of Mechanical and Electrical Engineering, Shihezi University, Shihezi 832003, China; 20192109022@stu.shzu.edu.cn (A.C.); yaoxuedong@126.com (X.Y.); liudecheng@stu.shzu.edu.cn (D.L.); lixiangyu@stu.shzu.edu.cn (X.L.); liyican@stu.shzu.edu.cn (Y.L.)
2 Ministry of Agriculture in Northwest China Key Laboratory of Agricultural Equipment, Shihezi 832003, China
3 College of Engineering, China Agricultural University, Beijing 100083, China; xhwcaugxy@163.com
* Correspondence: zx_mac@shzu.edu.cn

Abstract: The main objective of the present work was to study the drying kinetics and obtain the optimum process parameters of cantaloupe slices using short-and medium-wave infrared radiation (SMIR) drying technology. The effect of three independent variables of infrared radiation temperature (55–65 °C), slice thickness (5–9 mm) and radiation distance (80–160 mm) on the *L* value, color difference (ΔE), hardness and vitamin C content were investigated by using the Response Surface Methodology (RSM). The results showed that the Page model can adequately predict the moisture content between 55 and 65 °C ($R^2 > 0.99$). The effective moisture diffusivity (D_{eff}) varied from 5.26×10^{-10} to 2.09×10^{-9} m^2/s and the activation energy (Ea) of the SMIR drying was 31.84 kJ/mol. Infrared radiation temperature and slice thickness exerted extremely significant effects on *L* value and color difference (ΔE) ($p < 0.01$), with higher infrared radiation temperature and thin slice thickness leading to a decrease in the *L* value and an increase in ΔE. Hardness and vitamin C content were significantly affected by infrared radiation temperature, slice thickness and radiation distance, of which the slice thickness was the most distinct factor affecting the hardness value. Higher infrared radiation temperature and larger slice thickness and radiation distance resulted in higher vitamin C degradation. For the given constraints (maximized vitamin C content and *L* value, minimized ΔE and hardness value), the optimum drying parameters were infrared radiation temperature 58.2 °C, slice thickness 6 mm and radiation distance 90 mm. Under the optimum drying combination conditions, the experimental values were 65.58 (*L* value), 8.57 (ΔE), 10.49 N (hardness) and 106.58 mg/100 g (vitamin C content), respectively. This study is beneficial to the development of the cantaloupe food processing industry and provides more insights for the application of SMIR drying technology to improve the drying rate and product quality of cantaloupe.

Keywords: infrared drying; cantaloupe slice; kinetics; quality evaluation; optimization; texture; vitamin; color

1. Introduction

Cantaloupe (*Cucumis melon var. reticulatus.* Hami-melon) is a commercially valuable seasonal specialty fruit grown in northwest China and is rich in variety of vitamins, minerals and other antioxidant active ingredients [1]. These antioxidants play an essential role in inhibiting free radicals, preventing and repairing cellular damage in the body [2]. In addition, cantaloupe's unique aroma and juicy, sweet taste make it make it more likely to be enjoyed by consumers. However, fresh cantaloupe features a short shelf-life of about 15 days due to its high moisture content and perishability [3]. In addition, it is easily damaged during the process of picking and distribution, leading to mold contamination and serious economic losses, especially during long-distance transportation from Xinjiang to

the southeast provinces of China [1]. For most fruits and vegetables, drying is an important and common method to extend shelf life and reduce post-harvest losses. However, the prolonged drying of cantaloupe slices under high temperature and aerobic conditions will produce off-flavors, surface hardening, browning and the degradation of vitamins and other nutrients. In addition, cantaloupe pulp contains a large amount of sugar, which is absorbent for moisture molecules, leads to difficulty in dehydration and prolonged drying time [4]. Therefore, a fast and efficient drying method is imperative to shorten the drying time and reduce the changes in nutritional quality of cantaloupe slices.

Short- and medium-wave infrared radiation (SMIR) drying is a promising drying method. Compared with far-infrared drying (4–100 μm), SMIR drying (0.75–4 μm) features a greater penetration depth and higher radiation frequency, which is consistent with the absorption peak of water molecules and is more conducive to removing moisture inside the material [5,6]. Furthermore, SMIR drying offers significant advantages in terms of drying rate, energy efficiency and final product quality compared to conventional hot air drying. As a high heat transfer coefficient and environmentally friendly drying technology, SMIR drying has been successfully applied to various food products such as: carrot slices [7], jujube slices [8], sponge gourd slices [5], kiwifruit Slices [9], jujube Powder [10], red pepper [11] and quince slices [12].

During the drying process, the intrinsic quality characteristics (texture, flavor, aroma), sensory characteristics (color, shape, size) and nutritional value of fruit and vegetable products change [13,14]. These characteristics variations feature a very high consumer acceptance for commercial production. In recent years, studies on cantaloupe have mainly focused on texture characteristics (sensory and physical-chemical evaluation) [15], fresh-cut shelf-life [3] and cantaloupe juice sterilization [16], with some scholars studying the spray drying and foam drying of cantaloupe juice powder [2,17,18]. However, in these studies, limited scientific research related to SMIR drying kinetics and process parameter optimization of cantaloupe slices.

Drying kinetics is very useful for the optimization of process parameters, product quality improvement and heat and mass transfer in the drying process. Response surface analysis (RSM) is a universal tool to obtain the optimal production process parameters for the product, and can also be applied to investigate the effects among experimental variables and to model and analyze the optimization process. Therefore, the purpose of this paper is to study the drying kinetics, effective moisture diffusivity, thin-layer drying models under different radiation temperatures as well as activation energy, and focuses on determining the optimal SMIR drying process parameters for high-quality cantaloupe slices by analyzing the effects of different radiation temperatures, slice thicknesses and radiation distances on the L value, ΔE, hardness and vitamin C content using RSM.

2. Materials and Methods

2.1. Materials

The fresh cantaloupes (variety Xizhoumi No.17) without injuries that were used in this study were purchased from the local market (Shihezi City, China) and cold-stored in a refrigerator (4 ± 1 °C). The same batch samples were carefully selected to ensure uniform sizes and weights (the average length, diameter and weight were 30.81 ± 0.24 cm, 16.34 ± 0.18 cm and 4.15 ± 0.35 kg, respectively). The moisture content of fresh cantaloupe slices was calculated by using the hot air oven method (DHG-9070A, Yiheng Scientific Instrument Co., Ltd. Shanghai, China, accuracy of ±0.1 °C) at 105 °C for 24 h [19]. The average initial moisture content of the cantaloupes used in this study was 90.21% (wet basis) or 9.21 kg/kg (dry basis). Before the drying process, the sample was washed, peeled, deseeded and sliced into 30 × 50 × (5~9) mm-thin slices. Several measurements were taken for each sample using a caliper to obtain the required thickness.

2.2. Cantaloupe Slices SMIR Drying

The cantaloupe slices were dried in a triple-tray laboratory-scale SMIR dryer (STC, Taizhou Senttech Infrared Technology Co., Ltd., Jiangsu, China; temperature accuracy of ± 0.1 °C). The schematic diagram of the dryer is shown in Figure 1. The distances between the infrared radiation tubes and the material tray were 80, 120 and 160 mm, respectively. Six quartz glass infrared tubes were parallel to the material tray and the radiation power of three medium-wave (2–4 µm) and three short-wave (0.75–2 µm) infrared radiation tubes was 450 W, 225 W, 225 W, 450 W, 450 W and 225 W, respectively. The hot air flow was released vertically onto the material surface through 18 circular nozzles with a diameter of 10 mm uniformly distributed on the top of the drying chamber. During the drying experiment, four infrared tubes with a total radiation power of 1350 W were selected and the air velocity at the surface of the material in the drying chamber was kept constant at 2.35 ± 0.15 m/s (TES-1304, TES Electronics Industry Co., Ltd. Taiwan, China; accuracy of ± 0.01 m/s). A thermal sensor was used to measure and control the air temperature above the material tray. The temperature for the drying experiment was entered on the touch screen and the cantaloupe slices (approximately 300 g) were spread evenly in a single layer on the tray with a size of 42 × 35 cm. Before loading the samples, the dryer reached the steady state for the desired temperatures. To determine the moisture loss during the drying process, a digital balance with a resolution of 0.01 g (BSM-4200.2, Zhuojing Electronic Technology Co., Ltd. Shang Hai, China) was used to measure the weight of the product every 15 min, until achieving the equilibrium moisture content [20,21]. The dried samples were cooled and vacuum-packed (JBDZQ-6001D, Jiubo Machinery Equipment Co., Ltd. Zhengzhou, China) for further analysis.
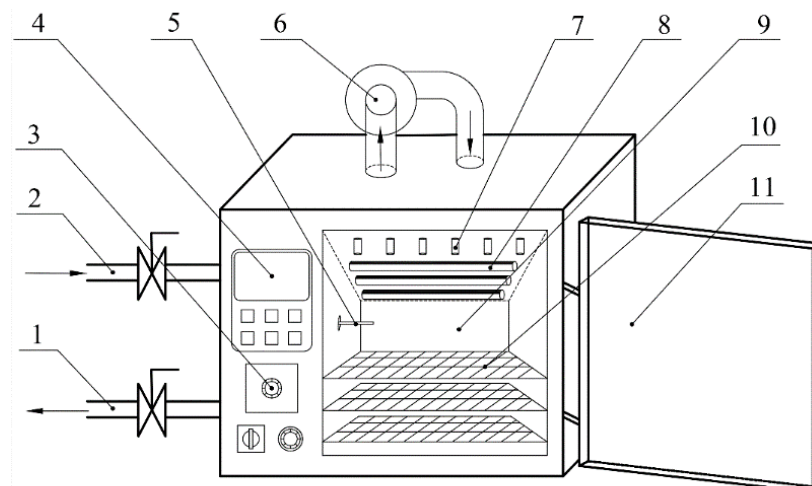
Figure 1. Schematic of the short- and medium-wave infra-red dryer. 1. wet discharging port, 2. air inlet port, 3. wind speed adjusting knob, 4. touch screen, 5. temperature sensor, 6. centrifugal fan, 7. spray nozzle 8. quartz infrared heating tube, 9. drying chamber, 10. material tray, 11. door.

2.3. Drying Characteristic Analysis

2.3.1. Calculation of Moisture Ratio and Drying Rate

The moisture ratio (MR) and drying rate (DR) were calculated using Equations (1) and (2), respectively [22,23].

$$\text{MR} = \frac{M_t - M_e}{M_0 - M_e} \tag{1}$$

where M_0, M_e represents the initial and equilibrium moisture content and M_t is the moisture content at time t (g/g dry basis):

$$DR = \frac{M_t - M_{t+\Delta t}}{\Delta t} \tag{2}$$

where M_t and $M_{t+\Delta t}$ represents the moisture content (g/g dry basis) at times t and t + Δt, respectively and t is time (min).

Furthermore, five empirical (Newton, Page, Henderson and Pabis, Midilli and others and two-term exponential model) drying models were selected and detailed in Table 1 to represent the drying characteristics of the cantaloupe slices during the SMIR drying process.

Table 1. Thin-layer empirical models applied to SMIR drying curves.

Model Number	Model Name	Model Equation	Reference
1	Newton model	$MR = \exp(-kt)$	[13]
2	Page model	$MR = \exp(-kt^n)$	[23]
3	Henderson and Pabis model	$MR = a\exp(-kt)$	[24]
4	Midilli and others model	$MR = a\exp(-kt)\,bt$	[25]
5	Two-term exponential model	$MR = a\exp(-k_1 t) + b\exp(-k_2 t)$	[8]

Note: MR, moisture ratio; a, b, n, k, k_1 and k_2, model constants; t, time (h).

2.3.2. Calculation of Effective Moisture Diffusivity and Activation Energy

In general, diffusion is regarded as the governing mechanism of moisture movement in fruit and vegetables and Fick's second law of diffusion is often considered to describe the moisture diffusion during the falling rate period [11,25]. Fick's diffusion equation be given as Equation (3) and can be used to calculate the relationship between MR and D_{eff} [23,26].

$$MR = \frac{8}{\pi^2} \exp\left(-\frac{\pi^2 D_{eff} t}{4L^2}\right) \tag{3}$$

where D_{eff} is the effective moisture diffusivity (m^2/s), t is the drying time (s), L is the half-thickness of cantaloupe slices (m). Equation (3) could be rewritten as:

$$D_{eff} = L^2 \times (-0.101 ln MR - 0.0213)/t \tag{4}$$

The D_{eff} of the cantaloupe slices at different temperatures can be described by Equation (5), as follows [8,26].

$$D_{eff} = D_0 \exp\left[-\frac{E_a}{R(T + 273.15)}\right] \tag{5}$$

where D_0 is the constant diffusivity factor (m^2/s); E_a is the activation energy (kJ/mol); R is the universal gas constant $\left(8.31 \text{ J mol}^{-1} \text{ K}^{-1}\right)$ and T is the drying temperature (°C).

The activation energy (E_a) was estimated from the slope of $ln D_{eff}$ versus $(1/(T + 273.15))$ as expressed in Equation (6).

$$ln D_{eff} = ln D_0 - \frac{E_a}{R} \frac{1}{(T + 273.15)} \tag{6}$$

2.4. Quality Parameters
2.4.1. Color

The surface color of the fresh and dehydrated cantaloupe slices was measured using a chroma meter (Type CR-410, Konica Minolta Inc., Tokyo, Japan) with a D_{65} standard illuminant and an observation angle of approximately 2°. Before each color measurement, the instrument was calibrated with a standard black-and-white plate. The color parameters L^* were defined as lightness and darkness, a^* as redness and greenness, and b^* as yellowness and blueness. The total color difference (ΔE) of dehydrated cantaloupe slices relative to the original cantaloupe slices was computed by Equation (7) [27].

$$\Delta E = \sqrt{\left(L^* - L_0^*\right)^2 + \left(a^* - a_0^*\right)^2 + \left(b^* - b_0^*\right)^2} \tag{7}$$

where L^*, a^* and b^* were the color parameters of dehydrated cantaloupe slices and the average values of L_0^*, a_0^* and b_0^* of the fresh cantaloupe slices were 72.02, 9.06 and 31.07, respectively.

2.4.2. Hardness

The hardness of the cantaloupe slices, which was defined as the maximum force of the force-deformation curve, was determined by a texture analyzer (TA. XT Plus, Stable Micro System, Ltd., Surrey, UK), According to the compressive test method described by Supmoon and Noomhorm [28] the dehydrated cantaloupe slices were placed on a hollow flat base, and a cylindrical probe (P2), with a constant speed of 2 mm/s, was used to apply direct force to the sample surface until the sample cracked.

2.4.3. Vitamin C Content

The 2,6-dichloroindophenol titrimetric method [29] was used to determine the vitamin C content of the dehydrated cantaloupe slices. Accurately weigh (10 g) of crushed cantaloupe sample (BSM-220.4, Zhuojing Electronic Technology Co., Ltd. Shang Hai, China; accuracy of ± 0.0001 g). Add a small amount (10 mL) of oxalic acid solution (20 g/L) and grind thoroughly, dilute to 100 mL, then titrate with the calibrated 2, 6-dichloro-indoxyl solution to pink without fading within 15 s. Record the consumed titration solution and repeat three times. The resultant vitamin C content was expressed as mg/100 g of cantaloupe powder.

2.5. Experimental Design

Researchers have found that the level of infrared radiation temperature, the thickness of the slices, and the distance between the infrared radiation emitter and the sample surface affect the color, hardness and nutrient retention of the product during the infrared radiation drying process [5,30]. Based on the material characteristics of the cantaloupe slices and the preliminary experiments, the radiation temperature X_1 (55, 60 and 65 °C), slice thickness X_2 (5, 7 and 9 mm) and radiation distance X_3 (80, 120 and 160 mm) were the independent variables in this design. The response variables were L value (Y_1), ΔE (Y_2), hardness (Y_3) and vitamin C content (Y_4). According to the Box–Behnken central combined experimental design principle, a total of 17 sets of experiments were carried out, in which the central test was repeated five times. The common second-order polynomial response surface model (Equation (8)) was employed to fit the experimental data to describe the relationship between each response and the independent variables [22,31].

$$Y = \beta_0 + \beta_1 X_1 + \beta_2 X_2 + \beta_3 X_3 + \beta_{11} X_1{}^2 + \beta_{22} X_2{}^2 + \beta_{33} X_3{}^2 + \beta_{12} X_1 X_2 \\ + \beta_{13} X_1 X_3 + \beta_{23} X_2 X_3 \tag{8}$$

Y is the response function for each response variable (Y_1–Y_4). β_0 is the constant terms. β_1, β_2 and β_3, are the linear coefficients. β_{11}, β_{22} and β_{33} are the quadratic coefficients. β_{12}, β_{13} and β_{23} are the interaction coefficients.

2.6. Statistical Analysis

All the samples were carried out in triplicate and all the data of the experiments were analyzed by statistical software SPSS (Version 21.0, SPSS Inc., Chicago, IL, USA). The results of the experiments were expressed as mean $\pm$ standard deviation. Analysis of variance (ANOVA) was used to find the significant terms of each response in the model and values of $p \leq 0.05$ were considered statistically significant. The software, Design Expert Ver. 7.1.0 (Stat-Ease 2009), was used to generate three-dimensional (3D) response surface graphs and optimize the SMIR drying process. Three statistical parameters (the coefficient of determination (R^2), reduced chi-square (χ^2) and root-mean-square error (RMSE)) for the

mathematical modeling of the food drying were used to evaluate the fitting quality of the model. These parameters were calculated from the following equations [13,32].

$$R^2 = 1 - \frac{\sum_{i=1}^{N} (MR_{pre,i} - MR_{exp,i})^2}{\sum_{i=1}^{N} (\overline{MR}_{pre} - MR_{exp,i})^2} \tag{9}$$

$$RMSE = \left[\frac{1}{N} \sum_{i=1}^{n} (MR_{pre,i} - MR_{exp,i})^2 \right]^{1/2} \tag{10}$$

$$\chi^2 = \frac{\sum_{i=1}^{N} (MR_{exp,i} - MR_{pre,i})^2}{N - n} \tag{11}$$

where $MR_{exp,i}$ and $MR_{pre,i}$ are the experimental and predicted data, respectively; N represents the number of data and n indicates model parameters.

3. Results and Discussion

3.1. Drying Kinetics and Modelling

The changing of the moisture ratio (MR) versus the drying time and the curve drying rate (DR) versus the moisture content under different infrared radiation temperatures of cantaloupe slices are shown in Figure 2. From Figure 2a, it can be observed that the moisture ratio decreased continuously with the extension of drying time; the infrared radiation temperature significantly affected the moisture ratio change and decreased faster at a higher infrared radiation temperature. Previous studies reported a similar observation of moisture ratio including jujube slices, sweet potato, red pepper and carrot slices and [8,32–34]. As infrared radiation drying temperatures increased from 55 to 65 °C, the drying time required of the cantaloupe samples from the initial moisture content to 0.14 kg/kg (dry basis) was 390, 300 and 240 min, respectively. The drying time obtained with SMIR drying was more rapid than the conventional hot air drying of cantaloupe slices, which required more than 360 min at a hot air drying temperature of 60 °C [35]. This finding means that SMIR drying could rapidly remove the moisture content from the cantaloupe slices. As expected, the enhanced infrared radiation temperature led to a shorter cantaloupe slice drying time. The reason might be that when the samples were exposed to greater infrared radiation temperatures, the increased radiation heat transfer accelerated the evaporation and diffusion of moisture [6,24,32]. In addition, the contraction of the volume of the cantaloupe slices in the final stage of the drying process may have collapsed the cytoskeletal structure, increasing the resistance to the movement of water from the inner layer to the surface, causing the moisture ratio to become slower.

Figure 2b presents the curve drying rate (DR) versus the moisture content under different infrared radiation temperatures. From Figure 2b, it is apparent that the infrared radiation temperature exerted a significant effect on the drying rate and that no constant DR period was found during the whole SMIR drying process. This implies that diffusion was the dominant physical mechanism of moisture change during the drying process of cantaloupe slices. The increased infrared radiation temperature increased the moisture diffusion from the cantaloupe slices surface to the surroundings [23,32,36]. As shown in Figure 2b, when the moisture content dropped to 0.14 kg/kg (dry basis), the values of DR were 0.0103, 0.0142, 0.0209 g/g h at the temperatures of 55, 60, 65 °C in SMIR drying, respectively. The reason for the increased DR value might be that infrared radiation can penetrate the material, creating a greater temperature difference between the product and the surrounding air, while higher SMIR temperatures feature a higher heat flux, which can improve the heating efficiency of SMIR drying. This was consistent with the findings for the infrared drying of kiwifruit slices [23] and the short- and medium-wave infrared radiation drying of jujube slices [8].
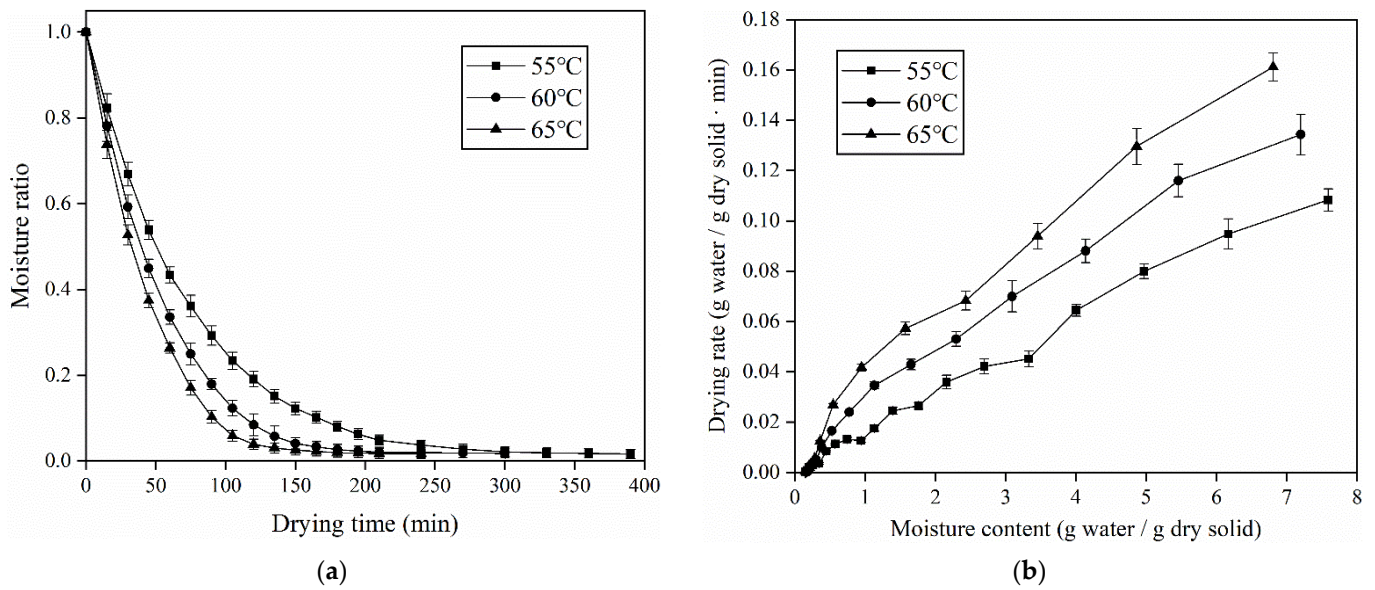
Figure 2. Moisture ratio (**a**) and drying rate (**b**) curves of cantaloupe slices under different SMIR drying temperatures (slice thickness 7 mm, radiation distance 120 mm).

In addition, the experimental data of the cantaloupe slice drying obtained at the different SMIR temperatures were converted into moisture ratio and fitted to five selected drying models to describe the drying characteristics of the cantaloupe slices. The statistical calculation results of the thin layer model selection criteria (R^2, RMSE and χ^2) and model constants (k, k_1, k_2, n, a and b) are shown in Table 2. Although all of the five selected models were a good fit for the experimental drying data, based on the highest R^2 (0.999), lowest RMSE (0.006~0.011) and χ^2 (3.108×10^{-5}~1.118×10^{-4}), the Page model could adequately describe the drying kinetics of the cantaloupe slices. Similar findings were reported by Fakhreddin and Maryam [37], who found that the Page model was suitable for predicting the drying kinetics of coated apple slices dried by infrared radiation. Pekke, et al. [27] also found that the Page model could adequately describe the infrared radiation drying characteristics of coated banana slices.

Table 2. Parameter values and statistical results of the thin layer drying models.

Model Number	Temperature (°C)	Model Parameters	R^2	RMSE	χ^2
	55	k = 0.807	0.999	0.008	6.874×10^{-5}
1	60	k = 1.120	0.997	0.015	2.336×10^{-4}
	65	k = 1.368	0.997	0.018	3.123×10^{-4}
	55	k = 0.821, n = 1.015	0.999	0.006	3.108×10^{-5}
2	60	k = 1.109, n = 1.099	0.999	0.009	7.275×10^{-5}
	65	k = 1.383, n = 1.118	0.999	0.011	1.118×10^{-4}
	55	a = 1.006, k = 0.831	0.999	0.008	3.278×10^{-5}
3	60	a = 1.021, k = 1.142	0.998	0.014	2.045×10^{-5}
	65	a = 1.020, k = 1.394	0.997	0.017	2.919×10^{-4}
	55	a = 1.008, b = 0.001×10^{-4}, k = 0.812	0.999	0.008	7.204×10^{-5}
4	60	a = 1.021, b = -1.469×10^{-4}, k = 1.141	0.998	0.015	2.180×10^{-5}
	65	a = 1.020, b = -5.771×10^{-4}, k = 1.389	0.997	0.018	3.128×10^{-4}
	55	a = 0.637, b = 0.369, k_1 = 0.831, k_2 = 0.831	0.999	0.006	3.663×10^{-5}
5	60	a = -0.570, b = 1.570, k_1 = 2.201, k_2 = 1.381	0.999	0.009	7.759×10^{-5}
	65	a = 0.368, b = 0.652, k_1 = 1.394, k_2 = 1.394	0.997	0.018	3.406×10^{-4}

Note: Drying process conditions: slice thickness 7 mm, radiation distance 120 mm. MR, moisture ratio; a, b, n, k, k_1 and k_2 model constants; t, time (h).

3.2. Effective Moisture Diffusivities and Activation Energy

The variation of effective moisture diffusivity (D_{eff}) values versus the moisture content (dry basis) of the cantaloupe slices at different SMIR temperatures is illustrated in Figure 3. At different infrared radiation temperatures, the D_{eff} value increases to its maximum as the moisture content (dry basis) decreases and decreases rapidly at the final drying stage. This behavior can be explained by the fact that at the initial stage of the drying process, infrared radiation heated the material in a relatively short time and the moisture molecules inside the cantaloupe slices were transferred to the surface of the material to evaporation, thereby increasing the D_{eff} value. In this stage, liquid and vapor diffusion was the dominant physical mechanism affecting moisture transport [33]. As the drying progressed to the later stage, the moisture content became lower and lower and the amount of steam decreased; furthermore, the shrinkage of the sample volume can further lead to D_{eff} value decreases during the final drying period [5]. The changes between the D_{eff} value and the moisture content were consistent with the research results reported by Chen et al. [8] with SMIR drying jujube slices and by Cao et al. [11], who used infrared drying on red peppers. From Figure 3, it can also be seen that the maximum values of D_{eff} at 55, 60 and 65 °C were 1.10×10^{-9}, 1.64×10^{-9}, 2.09×10^{-9} m²/s in SMIR drying, respectively. This shows that the temperature exerts a positive effect on the increase in the D_{eff} value during the whole drying process. This phenomenon mainly occurred because of the rapid heating by the infrared radiation and higher temperatures could increase the energy absorbed by water molecules and accelerate the diffusion of the moisture presented in the cantaloupe slices [5,11]. Chen et al. [8] stated that higher short- and medium-wave infrared radiation temperatures could lead to high vapor pressure inside the sample, thereby increasing the moisture diffusion of jujube slices, resulting in larger D_{eff} values.
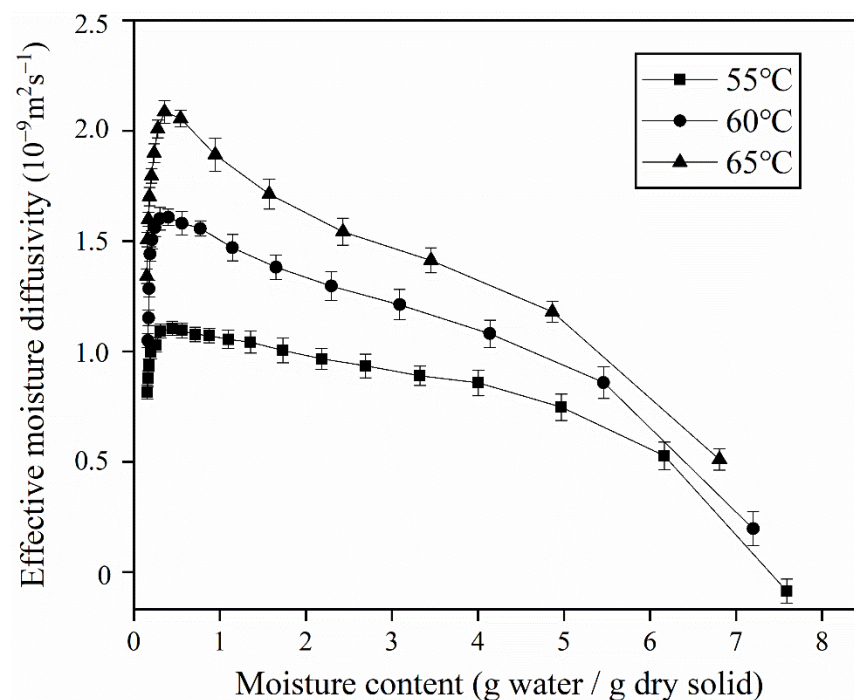
Figure 3. Effective moisture diffusivity versus moisture content of cantaloupe slices under different SMIR drying temperatures (slice thickness 7 mm, radiation distance 120 m).

The activation energy (*Ea*) of the cantaloupe slices was calculated from the slope of the Arrhenius function (Equation (6)) to be 31.84 kJ/mol. Table 3 lists the activation energy values of the cantaloupe slices and other agricultural products during infrared and infrared-assisted drying. As presented in Table 3, the *Ea* value of the cantaloupe slices was consistent with the activation energy of most infrared dried food and agricultural products

ranging from 12 to 70.2 kJ/mol [38]. Activation energy represents the energy required to remove moisture from the inside to the outside of the material, which is related to the specific surface area, structural properties and tissue components of the product. Generally, materials with high sugar or pectin content, dense tissue structure, few moisture migration channels and small specific surface areas feature higher *Ea* values [26,36].

Table 3. Activation energy of cantaloupe slices and other products during IR and IR-assisted drying.

Products	*Ea* (kJ/mol)	References
Cantaloupes slices	31.84	Present work
mushroom slices	21.85	Darvishi et al. [39]
Sour cherry	30.31–41.68	Chayjan, Kaveh, and Khayati. [40]
Pomegranate arils	30.80–37.48	Alaei and Chayjan. [41]
Red pepper	42.67	Cao et al. [11]
Kiwifruit slices	27.44	Lyu et al. [9]
Hazelnut kernel	33.02–50.22	Ghavidelan and Chayjan. [42]
Sweet potato slices	12.83–34.64	Onwude et al. [25]
Pumpkin slices	18.59–36.88	Sadeghi, Movagharnejad and Haghighi. [43]

3.3. Response Surface Methodology Optimization of Cantaloupe Slices

The independent variables and experimental data for the *L* value, Δ*E*, hardness and vitamin C content of cantaloupe slices under given different processing conditions are listed in Table 4. The ANOVA results of the respective regression models and model terms are presented in Table 5.

Table 4. Box–Behnken center design and results.

Run	Variables (Original and Coded Values)			Responses			
	X_1 (°C)	X_2 (mm)	X_3 (mm)	Y_1	Y_2	Y_3 (N)	Y_4 (mg/100 g)
1	55 (−1)	5 (−1)	120 (0)	63.15 ± 0.26	11.40 ± 0.03	9.88 ± 0.70	106.63 ± 2.27
2	65 (1)	5 (−1)	120 (0)	61.37 ± 0.25	15.21 ± 0.06	9.55 ± 0.46	88.53 ± 2.99
3	55 (−1)	9 (1)	120 (0)	62.07 ± 0.27	14.03 ± 0.20	15.58 ± 0.50	100.60 ± 3.14
4	65 (1)	9 (1)	120 (0)	53.53 ± 0.29	20.03 ± 0.35	13.86 ± 0.61	86.90 ± 4.54
5	55 (−1)	7 (0)	80 (−1)	64.03 ± 0.29	8.06 ± 0.25	11.49 ± 0.57	102.80 ± 3.33
6	65 (1)	7 (0)	80 (−1)	61.89 ± 0.29	12.86 ± 0.10	10.94 ± 0.74	91.60 ± 2.50
7	55 (−1)	7 (0)	160 (1)	63.36 ± 0.25	9.65 ± 0.13	12.68 ± 0.57	100.03 ± 2.48
8	65 (1)	7 (0)	160 (1)	60.29 ± 0.24	13.05 ± 0.11	12.21 ± 0.71	86.31 ± 3.24
9	60 (0)	5 (−1)	80 (−1)	65.86 ± 0.25	9.14 ± 0.07	9.12 ± 0.69	105.60 ± 3.59
10	60 (0)	9 (1)	80 (−1)	64.13 ± 0.36	13.51 ± 0.13	13.42 ± 0.67	99.87 ± 3.54
11	60 (0)	5 (−1)	160 (1)	65.49 ± 0.31	9.85 ± 0.04	10.01 ± 0.80	96.47 ± 3.36
12	60 (0)	9 (1)	160 (1)	60.48 ± 0.30	13.65 ± 0.06	14.62 ± 0.45	93.47 ± 2.19
13	60 (0)	7 (0)	120 (0)	63.40 ± 0.34	9.43 ± 0.15	11.79 ± 0.77	110.60 ± 1.85
14	60 (0)	7 (0)	120 (0)	65.74 ± 0.36	10.19 ± 0.11	12.25 ± 0.43	112.24 ± 2.19
15	60 (0)	7 (0)	120 (0)	64.46 ± 0.25	10.46 ± 0.02	12.33 ± 0.59	115.07 ± 3.26
16	60 (0)	7 (0)	120 (0)	64.82 ± 0.32	12.22 ± 0.14	12.04 ± 0.65	115.87 ± 2.56
17	60(0)	7 (0)	120 (0)	63.58 ± 0.27	12.06 ± 0.04	11.42 ± 0.70	112.15 ± 1.91

Table 5. ANOVA for respective regression models and model terms.

Source	df	Y_1 F Value	Y_1 p Value	df	Y_2 F Value	Y_2 p Value	df	Y_3 F Value	Y_3 p Value	df	Y_4 F Value	Y_4 p Value
Model	9	12.81	0.0014 **	9	15.19	0.0008 **	9	45.33	<0.0001 **	9	36.44	<0.0001 **
X_1	1	26.75	0.0013 **	1	44.07	<0.0003 **	1	9.72	0.0169 *	1	86.77	<0.0001 **
X_2	1	27.20	0.0012 **	1	33.15	0.0007 **	1	369.06	<0.0001 **	1	7.24	0.0310 *
X_3	1	4.39	0.0744	1	0.94	0.3646	1	21.34	0.0024 **	1	15.01	0.0061 **
$X_1 X_2$	1	10.14	0.0154 *	1	1.30	0.2911	1	3.98	0.0861	1	1.04	0.3408
$X_1 X_3$	1	0.19	0.6746	1	0.53	0.4892	1	0.013	0.9118	1	0.34	0.5767
$X_2 X_3$	1	2.39	0.1663	1	0.088	0.7750	1	0.20	0.6697	1	0.40	0.5462
X_1^2	1	33.26	0.0007 **	1	15.35	0.0058 **	1	0.73	0.4226	1	101.96	<0.0001 **
X_2^2	1	7.18	0.0316 *	1	27.79	0.0012 **	1	0.40	0.5484	1	43.59	0.0003 **
X_3^2	1	3.56	0.1011	1	14.80	0.0063 **	1	2.73	0.1423	1	49.84	0.0002 **
Lack of Fit	3	1.55	0.3325	3	0.11	0.9489	3	0.73	0.5844	3	0.90	0.5168
C.V. (%)		1.69			7.96			2.91			2.12	
R^2		0.9427			0.9513			0.9831			0.9791	
Adj-R^2		0.8691			0.8887			0.9614			0.9522	

Note: X_1—radiation temperature, X_2—slice thickness, X_3—radiation distance; Y_1—L value, $Y_2 \Delta E$, Y_3—hardness, Y_4—vitamin C content; * Significance at $p < 0.05$; ** significance at $p < 0.01$.

3.3.1. Influence of Variables on the Color of Cantaloupe Slices

Color is one of the important sensory qualities of dried products and has a significant impact on consumer choice and preference, as well as the marketing value of the product [44]. The second-order equation for the L value and ΔE value of the cantaloupe slices could be predicted by Equations (12) and (13).

$$Y_1 = -428.91 + 15.26X_1 + 15.24X_2 - 0.02X_3 - 0.17X_1X_2 - 1.16 \times 10^{-3}X_1X_3 \\ -0.01X_2X_3 - 0.12X_1^2 - 0.35X_2^2 + 6.10 \times 10^{-4}X_3^2 \tag{12}$$

$$Y_2 = 262.67 - 8.51X_1 - 10.72X_2 + 0.40X_3 + 0.05X_1X_2 - 1.75 \times 10^{-3}X_1X_3 \\ -1.78 \times 10^{-3}X_2X_3 + 0.07X_1^2 + 0.62X_2^2 - 1.12 \times 10^{-3}X_3^2 \tag{13}$$

As presented in Table 4, the L value and ΔE value of the final cantaloupe slices varied from 53.53 to 65.86 and from 8.06 to 20.03, respectively.

The correlation coefficients for the L value ($R^2 = 0.9427$, C.V.% = 1.69), for the ΔE ($R^2 = 0.9513$, C.V.% = 7.96) of the cantaloupe slices indicated that the regression equation was well fitted with the experimental data. According to the ANOVA results shown in Table 5, it can be seen that the L value of the cantaloupe slices was significantly ($p < 0.01$) affected by the linear term and quadratic term of the radiation temperature (X_1, X_1^2) and the linear term of slice thickness (X_2) and significantly ($p < 0.05$) affected by the interaction between radiation temperature and slice thickness ($X_1 X_2$) and the quadratic term of slice thickness (X_2^2). ΔE was significantly affected ($p < 0.01$) by the linear term and quadratic term of radiation temperature (X_1, X_1^2), slice thickness (X_2, X_2^2) and quadratic term of radiation distance (X_3^2). However, the mutual interaction between the three experimental variables ($X_1 X_2$, $X_1 X_3$, $X_2 X_3$) did not show any significant effect on the ΔE value in recent work.

The three-dimensional (3D) response surface graphs and perturbation plot for the effects of the variables on the L value of the cantaloupe slices is presented in Figure 4a–d. As shown in Figure 4a–c, the maximum L value was observed at $X_1 = 60\,°C$, $X_2 = 5$ mm and $X_3 = 80$ mm and the minimum value was found at $X_1 = 65\,°C$, $X_2 = 9$ mm and $X_3 = 120$ mm. The results of the perturbation plot (Figure 4d) showed that with the increasing radiation temperature (X_1) and slice thickness (X_2) (curve A and B in Figure 4d), the L value of the dehydrated product first increased and then decreased. The L value, that is, the whiteness or brightness of the final product, is closely related to the browning level: the lower its value, the more serious the browning reaction [27,45].
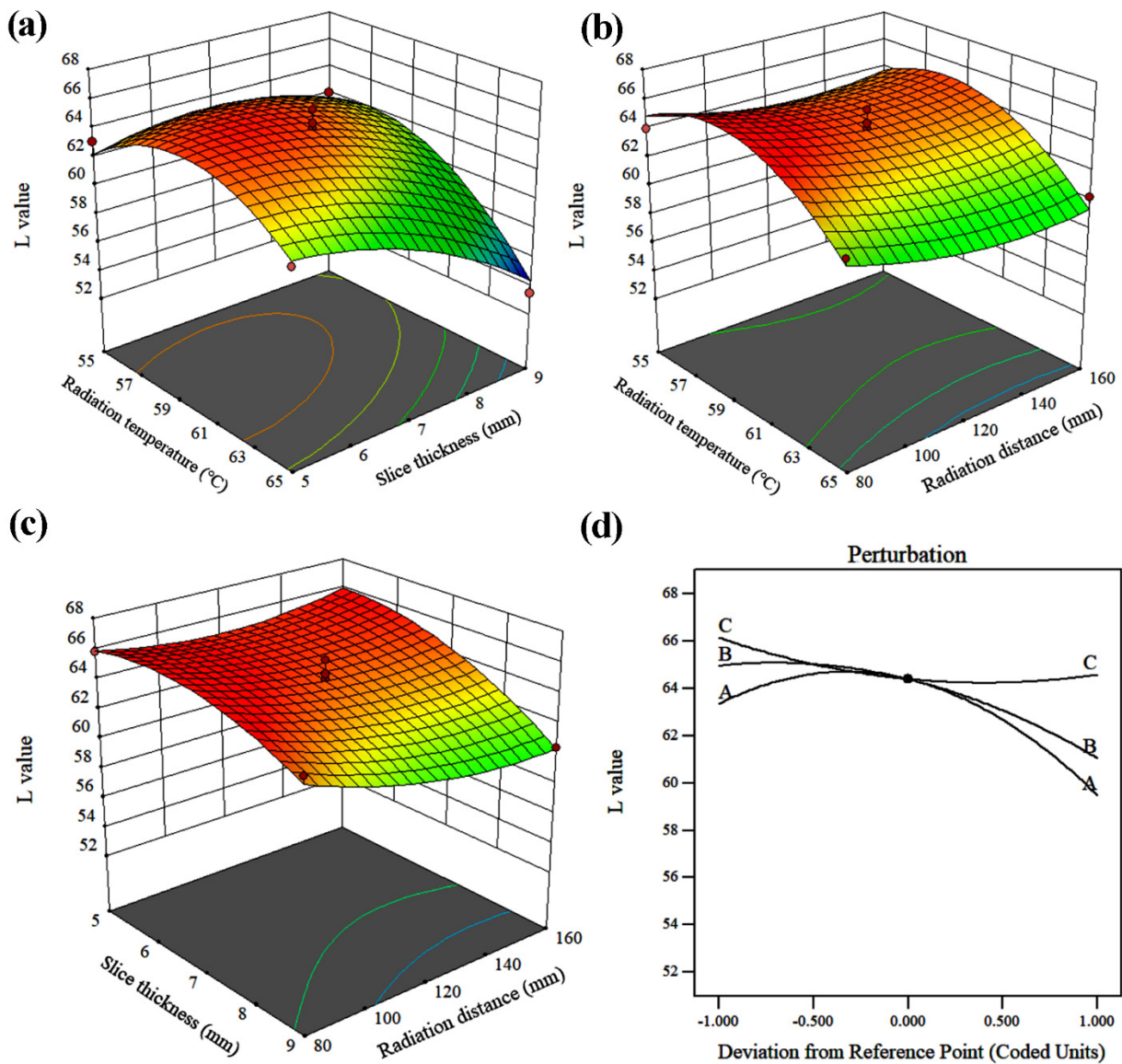
Figure 4. Response surface (**a**–**c**) and perturbation plot (**d**) for the effects of variables on the *L* value of cantaloupe slices.

Furthermore, from the perturbation plot (curve A in Figure 4d), when the infrared radiation temperature was higher than 60 °C, the *L* value decreased significantly with increasing radiation temperature. This phenomenon could be due to the fact that the fresh cantaloupe was rich in water and sugars; during the drying process with oxygen and high temperature, the reaction of reducing sugars and amino acids would generate dark components, which would decrease the *L* value of the product. The formation of brown products was also reported by Fang et al. [46], who reported that compared with dried at low temperatures (50 and 60 °C), high drying temperatures (70 °C) led to lower brightness of whole-fruit Chinese jujubes in hot-air drying. In addition, a similar phenomenon of brown pigment formation was found by Lyu et al. [9] for the SMIR radiation drying of kiwifruit slices and by Arslan and Özcan [47] for the oven drying (50 °C and 70 °C) of red bell peppers.

The response surfaces for the effects of the variables on the ΔE are shown in Figure 5a–c. It is clear from Figure 5a–c that the optimum conditions for the lowest value of ΔE were obtained at X_1 = 55 °C, X_2 = 7 mm and X_3 = 80 mm and that the highest values were obtained at X_1 = 65 °C, X_2 = 9 mm and X_3 = 120 mm. The results of the perturbation plot (Figure 5d) showed that the ΔE value first decreased and then increased with in-

creasing radiation temperature (X_1) and slice thickness (X_2) (curve A and B in Figure 5d). Thicker slices showed higher ΔE than thinner slices, which is consistent with the finding by Pekke, et al. [27] that more Maillard browning occurred in 8 mm-thick banana slices than in 5 mm-thick banana slices under the same infrared radiation heating. Zhang et al. [5] reported similar changes, in which thickness near to the infrared radiation penetration depth showed a significant effect in maintaining better color. Higher drying temperature induced greater ΔE, corresponding to heavier color deterioration in dried slices due to an increase in enzymatic browning [8,26]. This may be attributed to the fact that infrared radiation generates rapid and intense heat inside the material, causing serious damage to cell tissues, resulting in cell sap leakage, which increases the probability of contact between substrate with enzymes, causing enzyme browning and eventually leading a decrease in ΔE value. Furthermore, heat-sensitive components (vitamins, carotenes, carbohydrates and proteins) probably contributed to the surface color changes of the dried product [11,26].
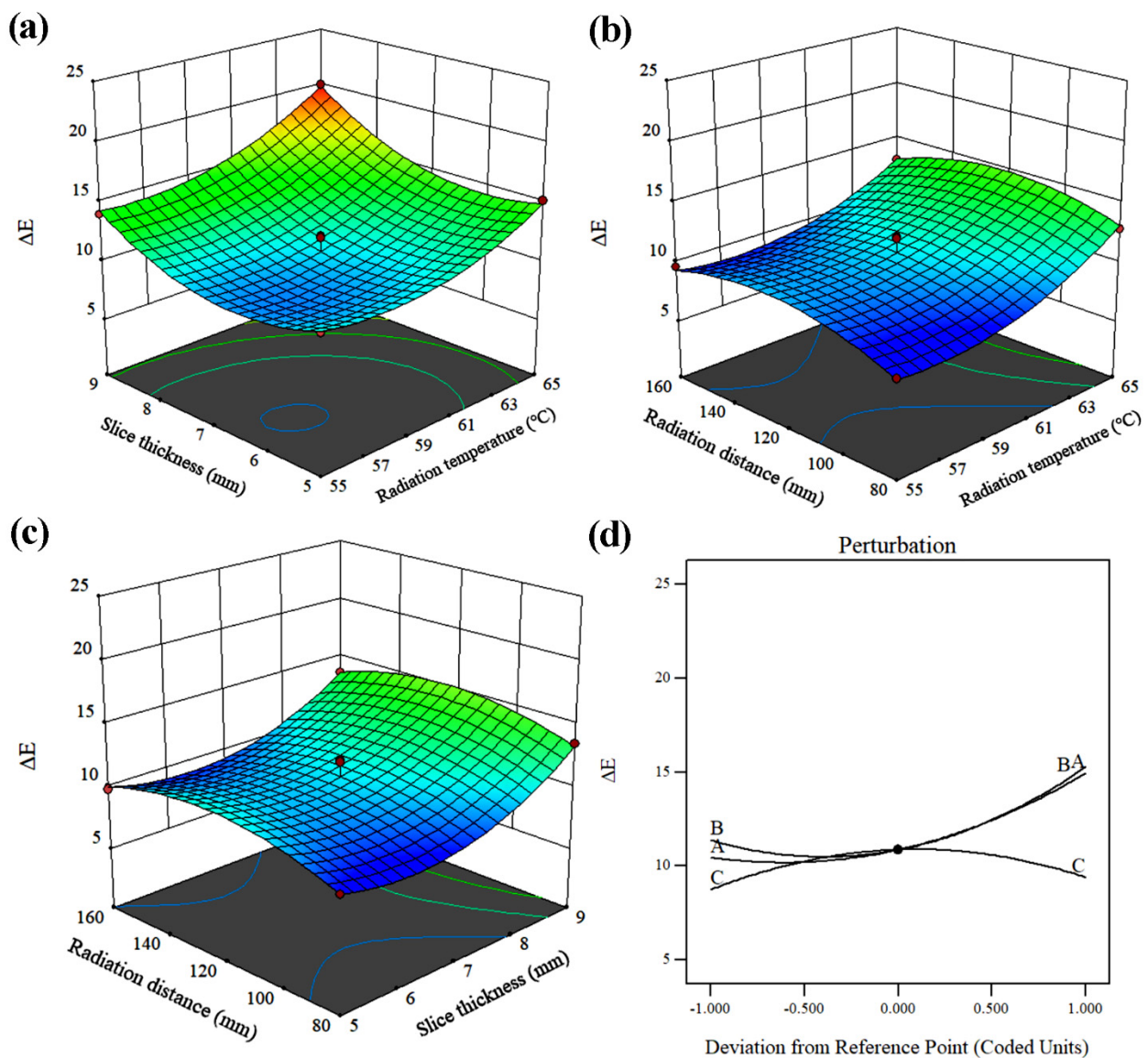
Figure 5. Response surface (**a**–**c**) and perturbation plot (**d**) for the effects of variables on the ΔE of cantaloupe slices.

3.3.2. Influence of Variables on the Hardness of the Cantaloupe Slices

The quadratic model for the hardness of the cantaloupe slices is represented by Equation (14):

$$Y_3 = 13.12 - 0.54X_1 + 2.78X_2 + 0.04X_3 - 0.03X_1X_2 + 1.00 \times 10^{-4}X_1X_3 + 9.69 \times 10^{-4}X_2X_3 + 5.78 \times 10^{-3}X_1^2 + 0.03X_2^2 - 1.75 \times 10^{-4}X_3^2 \tag{14}$$

From Table 5, results of the hardness ANOVA (R^2 = 0.9831, C.V.% = 2.91) showed that the obtained second-degree polynomial equation fitted the experimental data well. According to Table 5, the linear term of the slice thickness and radiation distance (X_2, X_3) reached an extremely significant level at $p < 0.01$; it was also significantly ($p < 0.05$) affected by the linear term of radiation temperature (X_1). However, the quadratic term (X_1^2, X_2^2 and X_3^2) and the mutual interaction among the three experimental variables were insignificant ($p > 0.05$) for hardness in this study. From the three-dimensional plot (Figure 6a–c), the highest hardness was obtained when X_1 = 55 °C, X_2 = 9 mm and X_3 = 120 mm, while when under the condition of X_1 = 60 °C, X_2 = 5 mm and X_3 = 80 mm, the hardness was the lowest. From the perturbation plot analysis (Figure 6d), the curve shape of the slice thickness (B line) was steeper than those of radiation temperature and radiation distance (A and C lines). This indicated that hardness was more sensitive to slice thickness than other variables. This means that the effect of slice thickness on hardness was the most significant variable: the larger the slice thickness value, the higher the hardness.

In addition, the higher radiation temperature and lower radiation distance led to a decrease in the hardness value. This may have been because infrared radiation can penetrate the material surface and directly heat the material from the inside; the higher infrared radiation energy forms a large temperature difference, which accelerates the diffusion of moisture from the material surface and produces a certain expansion, leading to a reduction in hardness. This phenomenon was similar to that observed by Supmoon and Noomhorm [28], who reported that due to the puffing caused by the rapid evaporation of water from inside the tissue by infrared absorption, the hardness decreased as the infrared intensity increased. Thuwapanichayanan, Prachayawarakorn, Kunwisawa and Soponronnarit [48] found that the banana slices dried at high temperature had more pore structures and smaller hardness values, compared with the samples dried at low temperature. Furthermore, Pei et al. [49] indicated that lower hardness values for infrared radiation dried samples with rapid evaporation of moisture caused swelling effects compared to hot-air dried samples. However, the opposite observation was reported by Guo et al. [50], who observed that with higher infrared heating power, a harder external layer was formed on the surfaces of carrot slices. The different changes of hardness can be attributed to the different materials, methods and parameters of drying used.
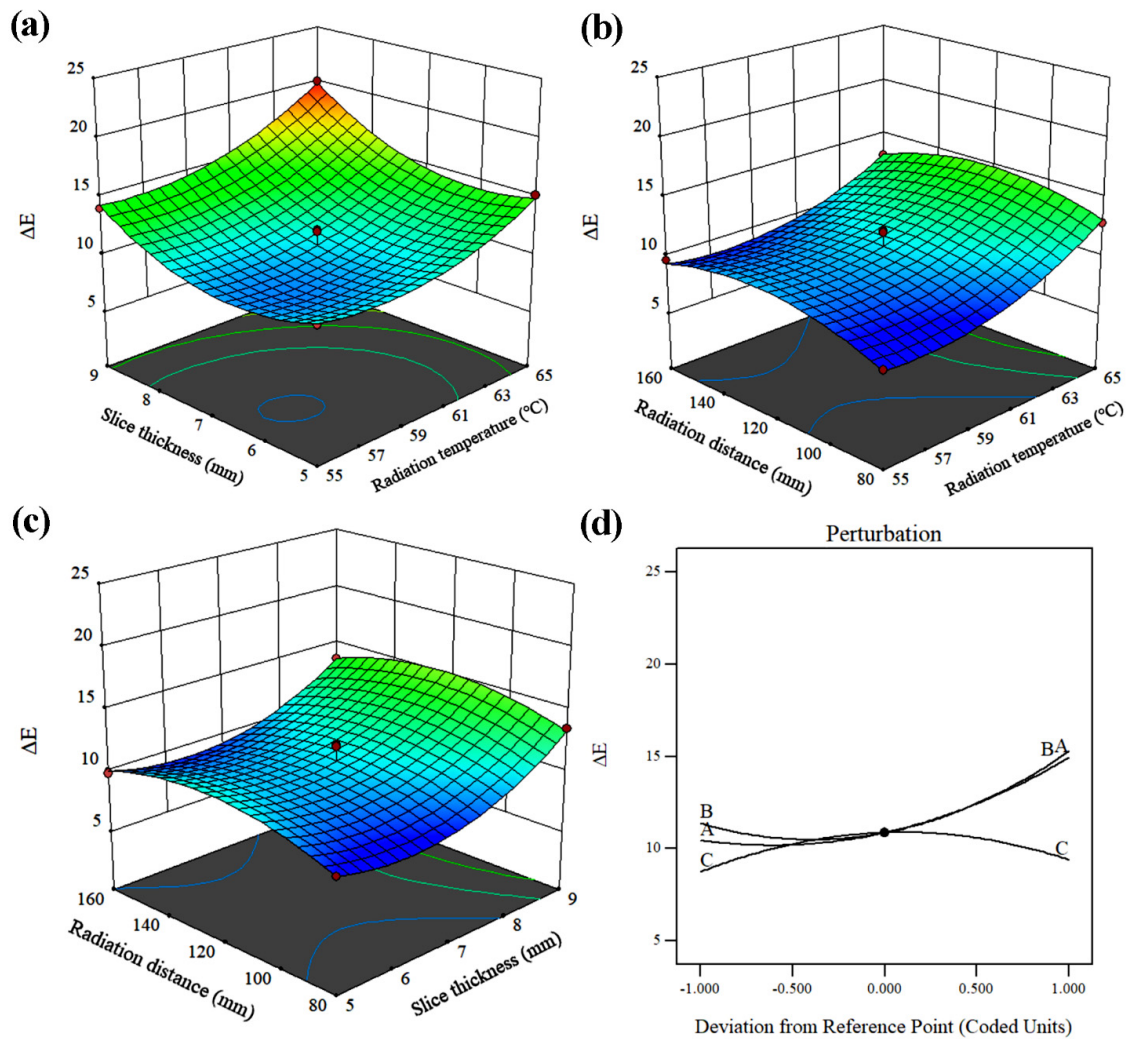
Figure 6. Response surface (**a**–**c**) and perturbation plot (**d**) for the effects of variables on the hardnessof cantaloupe slices.

3.3.3. Influence of Variables on the Vitamin C Content of the Cantaloupe Slices

Vitamin C is a natural, water-soluble antioxidant substance that is widely present in fruits and vegetables. Due to its low stability during thermal processing, it can be considered as a quality indicator of dried products [51]. The regression model for the vitamin C content of the cantaloupe slices is as follows:

$$
\begin{aligned}
Y_4 = &-1432.12 + 49.04X_1 + 15.60X_2 + 1.17X_3 + 0.11X_1X_2 - 3.15 \times 10^{-3}X_1X_3 \\
&+8.53 \times 10^{-3}X_2X_3 - 0.42X_1{}^2 - 1.73X_2{}^2 - 4.63 \times 10^{-3}X_3{}^2
\end{aligned}
\tag{15}
$$

From the results (Table 4), the vitamin C content was in the range of 86.31–115.87 mg/100 g. The ANOVA results indicated that the second-order equation fitted the present study well (R^2 = 0.9791, C.V.% = 2.12). The vitamin C content of the dried cantaloupe slices was significantly ($p < 0.01$) impacted by the quadratic terms of radiation temperature ($X_1{}^2$), slice thickness ($X_2{}^2$) and radiation distance ($X_3{}^2$), and the linear term of radiation temperature (X_1) and radiation distance (X_3). Moreover, the linear term of slice thickness (X_2) also exerted a significant effect at $p < 0.05$ (Table 5). However, the mutual interaction between the three experimental variables exerted non-significant effects on the vitamin C content. As shown in Figure 7a–c, the highest level of vitamin C content in the cantaloupe slices was around X_1 = 60 °C, X_2 = 7 mm X_3 = 120 mm; the lowest level was around X_1 = 65 °C, X_2 = 7 mm and X_3 = 160 mm. From the perturbation plot analysis (Figure 7d), the trend of vitamin C content first increased and then decreased with the increasing radiation

temperature (X_1), slice thickness (X_2) and radiation distance (X_3) (curves A, B and C in Figure 7d). When the drying temperature was higher than 60°C, the vitamin C content apparently decreased as the radiation temperature increased. This phenomenon was mainly due to the thermal sensitivity and instability of vitamin C, which was easy to degrade in drying processing, especially at high temperature. Chen et al. [8] reported that the increased drying temperature showed a significant effect on the decrease in vitamin C content in jujube slices, both in hot-air drying and short- and medium-wave infrared radiation drying. Similar trends have also been observed for other food materials, such as cantaloupe juice power [18], jujube powder [10] and blueberries [52]. In addition, the variation in vitamin C content was significantly affected by the slice thickness and radiation distance, probably because increases in slice thickness lead to longer drying times, prolonged exposure to excess oxygen heating can easily lead to vitamin C degradation and lower radiation distance causes water molecules within cantaloupe slices to absorb large amounts of infrared radiation energy in a short period of time, leading to increased volumetric heating; this in turn affects the temperature of the sample and drying time [5,18]. Zahoor and Khan [51] observed that using a lower drying temperature during the drying process required a longer drying time, which expedited the oxidation of vitamin C. Deng et al. [25] also found that the length of the processing time and drying temperatures were closely related to the oxidative degradation of vitamin C content.
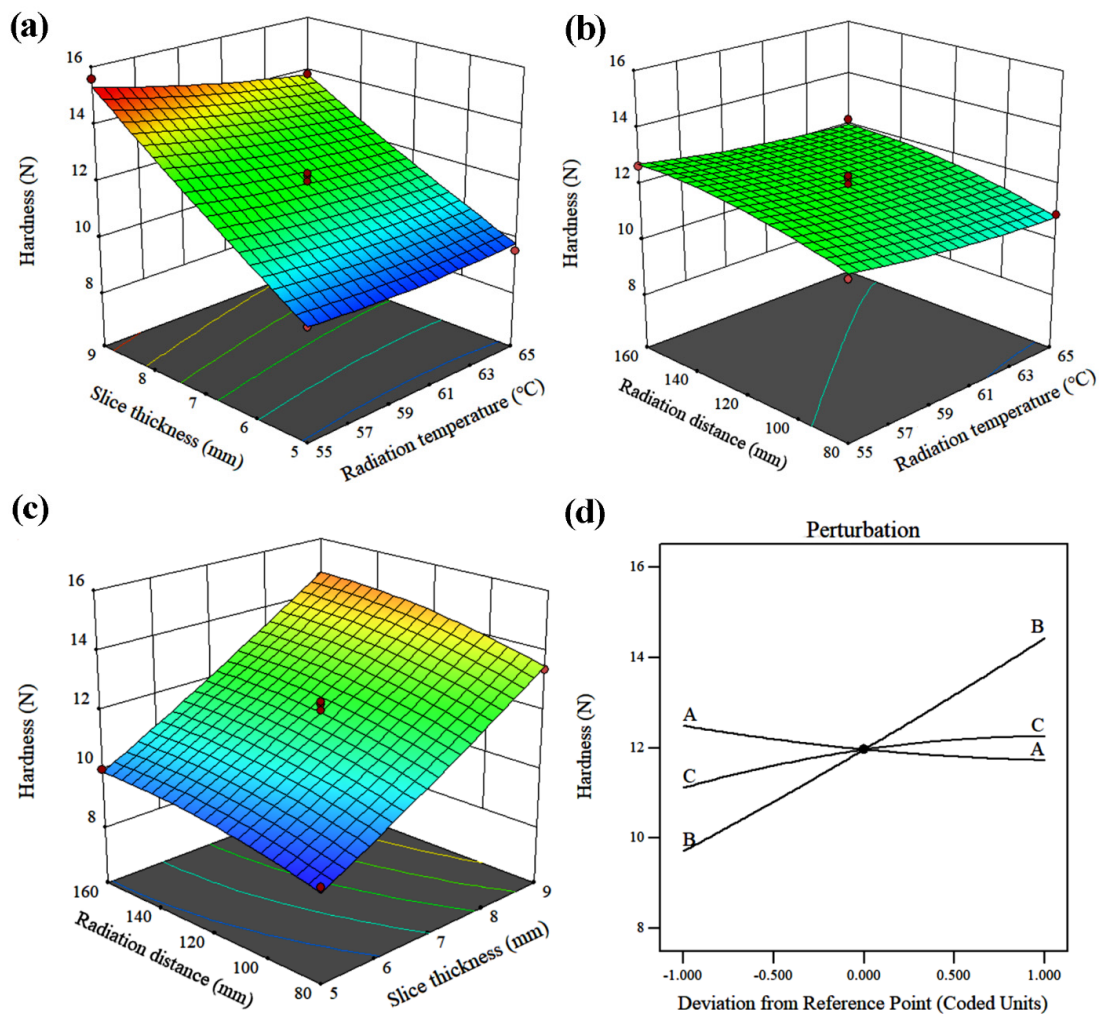
Figure 7. Response surface (**a**–**c**) and perturbation plot (**d**) for the effects of variables on the vitamin C content of cantaloupe slices.

3.4. Optimization and Verification

The radiation temperature, slice thickness and radiation distance were simultaneously optimized by a desirability function to obtain the optimum SMIR drying process parameters. The final objective was to obtain the minimum ΔE and hardness values of cantaloupe slices, as well as the maximum L value and vitamin C content. The numerical optimization of the optimum conditions for the SMIR drying process is shown in Table 6.

Table 6. Numerical optimization for optimum conditions.

Name	Goal	Lower Limit	Upper Limit	Importance
Radiation)	In range	55	65	3
Slice thickness (mm)	In range	5	9	3
Radiation distance (mm)	In range	80	160	3
L value	Maximize	53.53	65.86	4
ΔE	Minimize	8.06	20.03	4
Hardness (N)	Minimize	9.12	15.58	3
Vitamin C content (mg/100 g)	Maximize	86.31	115.87	5

The predicted optimum conditions were found to be radiation temperature (X_1) = 58.18 °C, slice thickness (X_2) = 5.88 mm and radiation distance (X_3) = 87.73 mm. To verify the reliability and adequacy of the predicted optimum results, considering the practical operation of the SMIR drying experiment, the best practical operating conditions and the final experimental values of L value, ΔE, hardness and vitamin C content under optimum conditions were shown in Table 6. The results indicated that the experimental values were in good consistent with the predicted values, with a relative error of less than 5% (Table 7). Therefore, the optimum conditions for dry cantaloupe slices by SMIR drying were as follows: radiation temperature, 58.2 °C; slice thickness, 6 mm; and radiation distance, 90 mm. Under these conditions, the response values for the L value, ΔE, hardness and vitamin C content were 65.58, 8.57, 10.49 N and 106.58 mg/100 g, respectively.

Table 7. Optimum conditions and verification test.

	X_1 (°C)	X_2 (mm)	X_3 (mm)	Y_1	Y_2	Y_3 (N)	Y_4 (mg/100 g)
Optimum condition	58.18	5.88	87.74	65.86	8.48	10.17	111.25
Verification test	58.2	6	90	65.58 ± 0.27	8.57 ± 0.13	10.49 ± 0.67	106.58 ± 2.35
Error (%)	-	-	-	0.43	1.06	3.15	4.20

Note: X_1—radiation temperature, X_2—slice thickness, X_3—radiation distance; Y_1—L value, Y_2 ΔE, Y_3—Hardness, Y_4—vitamin C content.

4. Conclusions

Short- and medium-wave infrared radiation (SMIR) drying was applied to dry cantaloupe slices in this study. The effects of radiation temperature (55–65 °C), slice thickness (5–9 mm) and radiation distance (80–160 mm) on the quality attributes (L value, ΔE, hardness and vitamin C content) of cantaloupe slices were studied using RSM and perturbation plot. The results showed that the Page model fitted well with the drying curves for the variation of the moisture ratio in the SMIR drying process. The values of effective moisture diffusivity varied from 5.26×10^{-10} to 2.09×10^{-9} m^2/s and increased significantly with increasing infrared radiation temperatures between 55 and 65 °C. The activation energy (Ea) of the cantaloupe slices was estimated as 31.84 kJ/mol.

Both infrared radiation temperature and slice thickness exhibited extremely significant effects on the color (L value and ΔE value) of the cantaloupe slices. The vitamin retention and hardness values were significantly affected by three independent variables (infrared radiation temperature, slice thickness and radiation distance). Among the three independent variables, the hardness values were most significantly influenced by the slice thickness and the vitamin C content showed a decreasing trend under higher infrared radiation temperatures, larger slice thickness and greater radiation distance. A regression analysis of the quadratic polynomial model indicated that the prediction models could represent the

experimental data adequately ($R^2 > 0.94$). By maximizing the vitamin C content and *L* value and minimizing the ΔE and hardness value, the optimal values for the SMIR drying process were determined: infrared radiation temperature of 58.2 °C, slice thickness of 6 mm and radiation distance of 90 mm. Based on the optimum drying parameters, the *L* value (65.58), ΔE (8.57), hardness value (10.49 N) and vitamin C content (106.58 mg/100 g) were simultaneously optimized.

These findings contribute to a better understanding of the drying characteristics of cantaloupe slices during SMIR drying and provide useful information for the selection of drying methods in the cantaloupe food processing industry. Moreover, by analyzing the effects of different process parameters on the quality characteristics of dried cantaloupe slices, the optimum SMIR drying conditions were determined. These are important for obtaining products with high nutritional quality and increasing the industrial added value of cantaloupe.

Author Contributions: Conceptualization, A.C. and X.Z.; methodology, A.C. and X.Z.; software, A.C., X.Z., H.X. and D.L.; validation, A.C. and X.Z.; formal analysis, X.Z., H.X. and A.C.; investigation, A.C., X.Z., D.L., Y.L. and X.L.; resources, A.C.; X.Z., H.X. and D.L.; data curation, A.C. and X.Z.; writing—original draft preparation, A.C.; writing—review and editing, A.C., X.Z., H.X., X.Y., D.L., Y.L. and X.L.; visualization, A.C. and X.Z.; supervision, X.Z., H.X. and X.Y.; project administration, X.Z. and X.Y.; funding acquisition, X.Z. and X.Y.; project administration, X.Z. and X.Y.; funding acquisition, X.Z. and X.Y. All authors have read and agreed to the published version of the manuscript.

Funding: This research was funded by the National Natural Science Foundation of China (Grant No. 31960488) and the Shihezi University Achievement Transformation and Technology Promotion Project (No. CGZH201808).

Institutional Review Board Statement: Not applicable.

Informed Consent Statement: Not applicable.

Data Availability Statement: All data used to support the findings of this study are included within the article.

Conflicts of Interest: The authors declare no conflict of interest.

References

1. Wen, X.; Hu, R.; Zhao, J.H.; Peng, Y.; Ni, Y.Y. Evaluation of the effects of different thawing methods on texture, colour and ascorbic acid retention of frozen hami melon (*Cucumis melo var. saccharinus*). *Int. J. Food Sci. Technol.* **2015**, *50*, 1116–1122. [CrossRef]
2. Li, T.S.; Rabiha, S.; Yaya, R.; Shazini, R. Effect of gum Arabic concentrations on foam properties, drying kinetics and physicochemical properties of foam mat drying of cantaloupe. *Food Hydrocoll.* **2021**, *116*, 106492. [CrossRef]
3. Martiñon, M.E.; Moreira, R.G.; Castell-Perez, M.E.; Gomes, C. Development of a multilayered antimicrobial edible coating for shelf-life extension of fresh-cut cantaloupe (*Cucumis melo* L.) stored at 4 °C. *Food Sci. Technol.* **2014**, *56*, 341–350. [CrossRef]
4. Salahi, M.R.; Mohebbi, M.; Taghizadeh, M. Development of cantaloupe (*Cucumis melo*) pulp powder using foam-mat drying method: Effects of drying conditions on microstructural of mat and physicochemical properties of powder. *Dry. Technol.* **2017**, *35*, 1897–1908. [CrossRef]
5. Zhang, Y.; Zhu, G.; Li, X.; Zhao, Y.; Lei, D.; Ding, G.; Ambrose, K.; Liu, Y. Combined medium- and short-wave infrared and hot air impingement drying of sponge gourd (*Luffa cylindrical*) slices. *J. Food Eng.* **2020**, *284*, 110043. [CrossRef]
6. Pawar, S.B.; Pratape, V.M. Fundamentals of infrared heating and its application in drying of food materials: A review. *J. Food Process Eng.* **2017**, *40*, e12308. [CrossRef]
7. Chen, Q.; Song, H.; Bi, J.; Chen, R.; Liu, X.; Wu, X.; Hou, H. Multi-objective optimization and quality evaluation of short- and medium-wave infrared radiation dried carrot slices. *Int. J. Food Eng.* **2019**, *15*, 20180234. [CrossRef]
8. Chen, Q.; Bi, J.; Wu, X.; Yi, J.; Zhou, L.; Zhou, Y. Drying kinetics and quality attributes of jujube (*Zizyphus jujuba Miller*) slices dried by hot-air and short- and medium-wave infrared radiation. *Food Sci. Technol.* **2015**, *64*, 759–766. [CrossRef]
9. Lyu, J.; Chen, Q.; Bi, J.; Zeng, M.; Wu, X. Drying characteristics and quality of kiwifruit slices with/without osmotic dehydration under short- and medium-wave infrared radiation drying. *Int. J. Food Eng.* **2017**, *13*, 1–15. [CrossRef]
10. Bi, J.; Chen, Q.; Zhou, Y.; Liu, X.; Wu, X.; Chen, R. Optimization of short- and medium-wave infrared drying and quality evaluation of jujube powder. *Food Bioprocess Technol.* **2014**, *7*, 2375–2387. [CrossRef]
11. Cao, Z.-Z.; Zhou, L.Y.; Bi, J.F.; Yi, J.Y.; Chen, Q.Q.; Wu, X.Y.; Zheng, J.K.; Li, S.R. Effect of different drying technologies on drying characteristics and quality of red pepper (*Capsicum frutescens* L.): A comparative study. *J. Sci. Food Agric.* **2016**, *96*, 3596–3603. [CrossRef]

12. Alaei, B.; Dibagar, N.; Chayjan, R.A.; Kaveh, M.; Taghinezhad, E. The effect of short and medium infrared radiation on some drying and quality characteristics of quince slices under vacuum condition. *Qual. Assur. Saf. Crops Foods.* **2018**, *10*, 371–381. [CrossRef]
13. Royen, M.J.; Noori, A.W.; Haydary, J. Experimental study and mathematical modeling of convective thin-layer drying of apple slices. *Processes* **2020**, *8*, 1562. [CrossRef]
14. Selvi, K.Ç.; Kabutey, A.; Gürkan, A.K.G.; David, H.; Kurhan, S.; Kloucek, P. The effect of infrared drying on color, projected area, drying time, and total phenolic content of rose (*Rose electron*) petals. *Plants* **2020**, *9*, 236. [CrossRef] [PubMed]
15. Farcuh, M.; Copes, B.; Le-Navenec, G.; Marroquin, J.; Jaunet, T.; Chi-Ham, C.; Cantu, D.; Bradford, K.J.; Van, D.A. Texture diversity in melon (*Cucumis melo* L.): Sensory and physical assessments. *Postharvest Biol. Technol.* **2020**, *159*, 111024. [CrossRef]
16. Fundo, J.F.; Miller, F.A.; Mandro, G.F.; Tremarin, A.; Brando, T.R.S.; Silva, C.L.M. UV-C light processing of Cantaloupe melon juice: Evaluation of the impact on microbiological, and some quality characteristics, during refrigerated storage. *Food Sci. Technol.* **2019**, *103*, 247–252. [CrossRef]
17. Tan, S.L.; Rabiha, S.; Yaya, R.; Shazini, R. Physical, chemical, microbiological properties and shelf life kinetic of spray-dried cantaloupe juice powder during storage. *Food Sci. Technol.* **2021**, *140*, 110597. [CrossRef]
18. Solval, K.M.; Sundararajan, S.; Alfaro, L.; Sathivel, S. Development of cantaloupe (*Cucumis melo*) juice powders using spray drying technology. *Food Sci. Technol.* **2012**, *46*, 287–293. [CrossRef]
19. AOAC. *Official Methods of Analysis of AOAC International*, 16th ed.; Association of Official Analytical Communities: Arlington, VA, USA, 1995.
20. Cunha, R.; Brandão, S.; Medeiros, R.; Júnior, E.; Silva, J.; Azoubel, P. Effect of ethanol pretreatment on melon convective drying. *Food Chem.* **2020**, *333*, 127502. [CrossRef]
21. Netto, J.; Honorato, F.; Azoubel, P.; Kurozawa, L.; Barbin, D. Evaluation of melon drying using hyperspectral imaging technique in the near infrared region. *Food Sci. Technol.* **2021**, *143*, 111092. [CrossRef]
22. Boateng, I.D.; Yang, X.M. Process optimization of intermediate-wave infrared drying: Screening by Plackett-Burman; comparison of Box-Behnken and central composite design and evaluation: A case study. *Ind. Crops Prod.* **2021**, *162*, 113287. [CrossRef]
23. Doymaz, I. Infrared drying of kiwifruit slices. *Int. J. Green Energy* **2018**, *15*, 622–628. [CrossRef]
24. Ferreira, J.; Queiroz, A.; Figueirêdo, R.; Silva, W.; Gomes, J.; Santos, D.; Silva, H.; Rocha, A.; Paiva, A.; Chaves, A.; et al. Utilization of Cumbeba (*Tacinga inamoena*) Residue: Drying Kinetics and Effect of Process Conditions on Antioxidant Bioactive Compounds. *Foods* **2021**, *10*, 788. [CrossRef] [PubMed]
25. Onwude, D.I.; Hashim, N.; Abdan, K.; Janius, R.; Chen, G. Modelling the mid-infrared drying of sweet potato: Kinetics, mass and heat transfer parameters, and energy consumption. *Heat Mass Transf.* **2018**, *54*, 2917–2933. [CrossRef]
26. Deng, L.Z.; Mujumdar, A.S.; Yang, W.X.; Zhang, Q.; Zheng, Z.A.; Wu, M.; Xiao, H.W. Hot air impingement drying kinetics and quality attributes of orange peel. *J. Food Processing Preserv.* **2020**, *44*, e14294. [CrossRef]
27. Pekke, M.A.; Pan, Z.L.; Atungulu, G.G.; Smith, G.; Thompson, J.F. Drying characteristics and quality of bananas under infrared radiation heating. *Int. J. Agric. Biol. Eng.* **2013**, *6*, 58–70.
28. Supmoon, N.; Noomhorm, A. Influence of combined hot air impingement and infrared drying on drying kinetics and physical properties of potato chips. *Dry. Technol.* **2013**, *31*, 24–31. [CrossRef]
29. AOAC. *Official Methods of Analysis of the Association of Official Analytical Chemists*; Official Method 967.21; AOAC International: Washington, DC, USA, 2000.
30. Sadeghi, E.; Movagharnejad, K.; Haghighi, A.A. Parameters optimization and quality evaluation of mechanical properties of infrared radiation thin layer drying of pumpkin samples. *J. Food Process Eng.* **2020**, *43*, e13309. [CrossRef]
31. Taghinezhad, E.; Kaveh, M.; Szumny, A. Optimization and prediction of the drying and quality of turnip slices by convective-infrared dryer under various pretreatments by RSM and ANFIS methods. *Foods* **2021**, *10*, 284. [CrossRef]
32. Onwude, D.I.; Hashim, N.; Abdan, K.; Janius, R.; Chen, G. The effectiveness of combined infrared and hot-air drying strategies for sweet potato. *J. Food Eng.* **2019**, *241*, 75–87. [CrossRef]
33. Deng, L.; Yang, X.; Mujumdar, A.S.; Zhao, J.; Wang, D.; Zhang, Q.; Wang, J.; Gao, Z.; Xiao, H.W. Red pepper (*Capsicum annuum* L.) drying: Effects of different drying methods on drying kinetics, physicochemical properties, antioxidant capacity, and microstructure. *Dry. Technol.* **2018**, *36*, 893–907. [CrossRef]
34. Wu, B.G.; Ma, H.L.; Qu, W.J.; Wang, B.; Zhang, X.; Wang, P.L.; Wang, J.; Atungulu, G.G.; Pan, Z. Catalytic infrared and hot air dehydration of carrot slices. *J. Food Process Eng.* **2014**, *37*, 111–121. [CrossRef]
35. Li, L.; Chen, J.; Duan, X.; Ren, G. Prediction model for moisture content in cantaloupe slices using LF-NMR and different drying methods. *Trans. Chin. Soc. Agric. Eng.* **2021**, *37*, 304–312. [CrossRef]
36. Xiao, H.W.; Pang, C.L.; Wang, L.H.; Bai, J.W.; Yang, W.X.; Gao, Z.J. Drying kinetics and quality of Monukka seedless grapes dried in an air-impingement jet dryer. *Biosyst. Eng.* **2010**, *105*, 233–240. [CrossRef]
37. Fakhreddin, S.C.; Maryam, S. Influence of infrared drying on drying kinetics of apple slices coated with basil seed and xanthan gums. *Int. J. Fruit Sci.* **2021**, *21*, 519–527. [CrossRef]
38. Delfiya, D.S.A.; Prashob, K.; Murali, S.; Alfiya, P.V.; Samuel, M.P.; Pandiselvam, R. Drying kinetics of food materials in infrared radiation drying: A review. *J. Food Process Eng.* **2021**, *1*, e13810. [CrossRef]
39. Darvishi, H.; Najafi, G.; Hosainpour, A.; Khodaei, J.; Aazdbakht, M. Far-infrared drying characteristics of mushroom slices. *Chem. Prod. Process Modeling* **2013**, *8*, 107–117. [CrossRef]

40. Chayjan, R.A.; Kaveh, M.; Khayati, S. Modeling some Drying Characteristics of Sour Cherry (*Prunus cerasus* L.) under Infrared Radiation Using Mathematical Models and Artificial Neural Networks. *Agric. Eng. Int. CIGR J.* **2014**, *16*, 265–279. Available online: https://cigrjournal.org/index.php/Ejounral/article/view/2552 (accessed on 1 January 2022).

41. Alaei, B.; Chayjan, R.A. Drying characteristics of pomegranate arils under near infrared-vacuum conditions. *J. Food Processing Preserv.* **2015**, *39*, 469–479. [CrossRef]

42. Ghavidelan, M.A.; Chayjan, R.A. Modeling engineering characteristics of hazelnut kernel during infrared fluidized bed drying. *J. Food Meas. Charact.* **2017**, *11*, 460–478. [CrossRef]

43. Sadeghi, E.; Movagharnejad, K.; Haghighi, A.A. Mathematical modeling of infrared radiation thin-layer drying of pumpkin samples under natural and forced convection. *J. Food Processing Preserv.* **2019**, *43*, e14229. [CrossRef]

44. Fatemeh, J.; Kamyar, M.; Ebrahim, S. Infrared drying effects on the quality of eggplant slices and process optimization using response surface methodology. *Food Chem.* **2020**, *333*, 127423. [CrossRef]

45. Wang, J.; Law, C.L.; Nema, P.K.; Zhao, J.H.; Liu, Z.L.; Deng, L.Z.; Gao, Z.J.; Xiao, H.W. Pulsed vacuum drying enhances drying kinetics and quality of lemon slices. *J. Food Eng.* **2018**, *224*, 129–138. [CrossRef]

46. Fang, S.Z.; Wang, Z.F.; Hu, X.S.; Datta, A.K. Hot-air drying of whole fruit Chinese jujube (*Zizyphus jujuba Miller*): Physicochemical properties of dried products. *Int. J. Food Sci. Technol.* **2009**, *44*, 1415–1421. [CrossRef]

47. Arslan, D.; Özcan, M.M. Dehydration of red bell-pepper (*Capsicum annuum* L.): Change in drying behavior, colour and antioxidant content. Food and Bioproducts Processing. *Trans. Inst. Chem. Eng.* **2011**, *89*, 504–513. [CrossRef]

48. Thuwapanichayanan, R.; Prachayawarakorn, S.; Kunwisawa, J.; Soponronnarit, S. Determination of effective moisture diffusivity and assessment of quality attributes of banana slices during drying. *Food Sci. Technol.* **2011**, *44*, 1502–1510. [CrossRef]

49. Pei, Y.S.; Li, Z.F.; Song, C.F.; Li, J.; Song, F.H.; Zhu, G.Y.; Liu, M.B. Effects of combined infrared and hot-air drying on ginsenosides and sensory properties of ginseng root slices (*Panax ginseng Meyer*). *J. Food Processing Preserv.* **2020**, *44*, e14312. [CrossRef]

50. Guo, Y.; Wu, B.; Guo, X.; Ding, F.; Pan, Z.; Ma, H. Effects of power ultrasound enhancement on infrared drying of carrot slices: Moisture migration and quality characterizations. *Food Sci. Technol.* **2020**, *126*, 109312. [CrossRef]

51. Zahoor, I.; Khan, M.A. Microwave assisted fluidized bed drying of red bell pepper: Drying kinetics and optimization of process conditions using statistical models and response surface methodology. *Sci. Hortic.* **2021**, *286*, 110209. [CrossRef]

52. Zielinska, M.; Markowski, M. The influence of microwave-assisted drying techniques on the rehydration behavior of blueberries (*Vaccinium corymbosum* L.). *Food Chem.* **2016**, *196*, 1188–1196. [CrossRef] [PubMed]